

Preparation and Characterization of Waterborne Polyurethane/Cellulose Nanocrystal Composite Membrane from Recycling Waste Paper

Xing Zhou^{1,*}, Xin Zhang¹, Dong Wang¹, Changqing Fang^{1,*}, Wanqing Lei¹, Zhigang Huang², Yonghua Song¹, Xinyu He¹ and Yingwei Huang¹

¹Faculty of Printing, Packaging Engineering and Digital Media Technology, Xi'an University of Technology, Xi'an, 710048, China

²School of Materials Science and Mechanical Engineering, Beijing Technology and Business University, Beijing, 100048, China

*Corresponding Authors: Xing Zhou. Email: zdxnlxaut@163.com; Changqing Fang. Email: fcqxaut@163.com

Received: 16 February 2020; Accepted: 14 April 2020

Abstract: Cellulose plays a key role in abundant organic natural materials meeting the increasing demand for green and biocompatible products. The highly crystalline nanoscale component of cellulose nanocrystals has recently attracted great attention due to the versatile performance as filler or matrix in producing functional materials. In this work, we prepared the waterborne polyurethane via a pre-polymer process, and obtained cellulose and cellulose nanocrystals from waste paper via a facile acid hydrolysis process. After that, the cellulose nanocrystals were assembled into film and mixed with polyurethane to prepare flexible polyurethane/cellulose nanocrystals composite membrane with different soaking time. The correlation between the bulk structure and applied properties including thermal resistance and mechanical property was investigated by using Fourier transform infrared spectroscopy (FTIR), X-ray diffraction (XRD), X-ray photoelectron spectroscopy (XPS), scanning electron microscopy (SEM), thermogravimetric analysis (TGA), differential scanning calorimetry (DSC) and folding test. The structure analysis indicates that cellulose nanocrystals prepared from used paper have a quality similar to that of commercial cellulose. Meanwhile, the cellulose nanocrystals have been mixed with polyurethane uniformly. Polyurethane can significantly benefit to the thermal resistance and mechanical property of the cellulose nanocrystals film. The polyurethane/cellulose nanocrystals composite membrane present good flexibility and may hold a significantly potential application as visual and flexible material.

Keywords: Cellulose; waterborne polyurethane; membrane; recycling

1 Introduction

In recent years, natural resources have attracted an increasing attention due to the high performance, renewability, degradation and biocompatibility [1–3]. Celluloses are one of the most important natural resources which mainly come from various animal and plant fibers including defatted rice bran, tunicate, algae, wood, pulp, cotton, asparagus and so on [4–11]. Recently, celluloses are commonly broken down to nanoscale via various physical and chemical methods with promising and wide applications [12,13]. Cellulose nanocrystals (CNC) are such significant nanocellulose with unique properties, such as high



This work is licensed under a Creative Commons Attribution 4.0 International License, which permits unrestricted use, distribution, and reproduction in any medium, provided the original work is properly cited.

specific strength and modulus, large surface area, high crystallinity and unique optical properties [14,15]. Actually, most of the recent researches focus on the preparation of CNC in different processes and resources [16] to enhance the nanostructure and performance and then to develop innovative high value polymers or composites with significant functionalities [17]. One of the most promising ways to produce CNC is to employ the cellulose generated from waste papers [18]. In this way, not only cellulose and cellulose nanocrystals can be obtained from waste paper, but also the wasting of paper resources may be significantly reduced.

However, some main shortcomings concerning the using of CNC as filler or matrix are their efficient fabrication with promising quantity and quality, as well as the brittleness. Meanwhile, the CNC filler or matrix is liable to be affected with damp [19]. It is reported that the acid hydrolysis is effective to obtain CNC in good quantity and quality with low cost [16]. Meanwhile, the employment of synthesized polymers is regarded as a promising way to improve the mechanical property and resistance to environment [20], even endowing the material to functionalities, such as shape memory, filterability and biocompatibility [6,21]. Thus, we assume that the combination of CNC with water-based polymer may present interesting properties.

Waterborne polyurethane (WPU) is a key water-based polymer whether in research or in industry. Polyurethane may be the only class of polymers that presents elastomeric, thermoplastic, and thermoset behavior. With the alternative hard- and soft-segment chains, the properties of polyurethane can be adjusted by using various components or different content of hard or soft segments [22]. Thus, it can be widely used in adhesives, coatings, printing and medicine areas [23]. In regarding to the chain structure of cellulose and WPU, both of them possess a large number of functional groups, holding promising and efficient way to interact with each other by connection of these functional groups. In our previous works, we have prepared various kinds of WPU and investigated the potential applications in printing ink and adhesion. We found that little attention has been paid to use polyurethane as modifying agent to increase the properties of CNC matrix. In this work, we implied that the employment of WPU to prepare WPU/CNC composite might present meaningful performance. Firstly, CNC was prepared by the sulfuric acid hydrolysis of the amorphous regions of waste paper and WPU was synthesized by the prepolymer process respectively according to our previous works [18]. Then, the WPU was dissolved in organic solvent to form solution as modified agent. Synchronously, the CNC dispersion was handled and dried in a facile way to form integrated CNC film. After that, the WPU was combined with CNC film in a spontaneous process with the variation of time. The correlation between the bulk structure of the WPU/CNC composite and the properties including thermal resistance and mechanical property are also investigated.

2 Experiments

2.1 Materials

Microcrystalline cellulose (MCC) was bought from Junkai Chemical, Zhengzhou, China. Office waste paper (OWP) was collected from our laboratory. Polypropylene glycol (PPG) (molecular weight $M_w = 2000$) was supplied by Sinopharm Chemical Reagent Co., Ltd. Isophorone diisocyanate (IPDI) (AR: Analytical reagent) was supplied by Aiaddin Industrial Corporation, Shanghai, China. Dibutyltin dilaurate (DBTDL) (CP) was obtained from Qingxi Chemical, Shanghai, China. Dimethylolpropionic acid (DMPA) was supplied by Xiangyang Chemical. 1-methyl-2-pyrrolidone (NMP) (AR) was obtained from Beilian fine Chemical, Tianjing, China. 1,4-Butanediol (BDO) (AR) was supplied by Fucheng Chemical Regent, Tianjing, China. Triethylamine (TEA) (AR) was bought from Fuyu fine chemical Regent, Tianjing, China. KOH (AR) was supplied by Tianjing Kermel Chemical Regent Co., Ltd. Hydrogen peroxide sulfuric acid (H_2SO_4) (GR: Guaranteed Regent, the purity of 59% (w/w)) was supplied by Tianli Chemical, Tianjing, China. Acetone (AR) was obtained from Haohua Chemical Regent Co., Ltd. In order

to reduce the viscosity, acetone was added during the whole process. All agents were used directly without any treatment except for PPG, which need to be dried in the oven.

2.2 Synthesis of Waterborne Polyurethane

WPU was prepared by prepolymer process. Firstly, 20 g PPG were added three necked glass reactor and then the three necked glass reactor was placed in the oven and reacted at 110°C for 2 h. The point of this step was to dry the PPG thoroughly. The PPG was mixed with 8.916 g IPDI in a three-necked glass reactor installed with mechanical stirrer, spiral condenser. And then the three-necked glass reactor was charged to an electric-heated thermostatic water bath and reacted for 2 h at 80°C, 250 r/min. After that catalyst DBTDL was put to the mixture and reacted for 30 min. Afterwards, 1.568 g DMPA and 2.563 g NMP was added to the mixture and reacted for 15 min, following by adjusting the revolving speed to 300 r/min when the temperature decreased to 60°C. Then, the reaction temperature was increased and kept at 80°C for 2 h. After the reaction between the isocyanate and polyols, the temperature was decreased to 40°C, and 0.86 mL 1,4-BDO was added to the glass reactor and reacted for 1 h. Finally, 30 g deionized water dispersed with a certain amount of TEA was added to the reactor and stirred under a strong agitation for 10 min to get a homogenous polyurethane dispersion. During this step, pH of the dispersion was adjusted to be 9–10 by adding a certain amount of KOH. The obtained WPU of 10 mL was poured into the polyfluortetraethylene plate, and dried in an oven at 50°C for 2–3 days.

2.3 Deinking and Defibering of OWP

According to our previous work [18], the cellulose fibers can be prepared from waste paper as the following processes. OWP (30 g) was collected from our laboratory and shredded into pieces of 15 mm × 4 mm by paper shredder. Then deinking agents including 1.5 wt% NaOH, 3 wt% H₂O₂, 5 wt% NaSiO₃, 1.5 wt% SDBS and 1.5 wt% OP-10 were dissolved in the tap water of 1000 ml and stirred by the glass rod. The prepared deinking agents and paper pieces were added into the laboratory repulper, and soaked for about half an hour. Afterwards, the repulper started to defibrize at the speed of 10000 r/min for approximately 10–15 min. In the cooperation of chemical agents and mechanical forces, the ink fell off the waste paper and the defibered paper was obtained. Subsequently, the defibered paper was washed for several times through a fine-mesh for the purpose of removing the ink and impurities from the OWP pulp. Finally, deinked office waste paper (OWP) pulp was dried in the oven at 80°C for 24 h and smashed with the high-speed universal pulverizer for 10–30 s to obtain fine deinked OWP pulp fibers (DP). Thus, the mechanical treatment resulted in disintegration of the cellulose structure into microcrystalline cellulose particles.

2.4 Preparation of Cellulose Nanocrystals Films

To recycle waste papers and save resources, the cellulose nanocrystal was extracted effectively and piled up via the filtration method. As a comparison, the commercial cellulose was also used as the nanocrystal resource. The cellulose nanocrystals were obtained from the collected waste paper reported in our previous work [18]. Firstly, the treated cellulose of 2 g was mixed with 48.43 mL H₂SO₄ (59% w/w) and deionized water of 58.89 g, which were stirred under a constant agitation of 270 r/min at 45°C for 1 h. Deionized water of 1 L was poured into a beaker and frozen for 1 h. Afterwards, the mixture was added to the cold water and stood 1 h to form a suspension liquid. Then, the mixture was washed for several times with water via a filtered washing process until the pH of the filtrate was neutral. In this way, the CNC was obtained after the water was removed. The CNC was collected and dispersed in deionized water under ultrasound condition of 200 W, 30 min with ice-bath. To tailor the weight fractions of the CNC films from different celluloses to exactly the same values, the CNC from different resources in the same weight was dispersed [24]. Once again, the air pump filtration process was carried out to remove water and array the CNC to obtain the films. Finally, the films were dried in an oven at 50°C for 8 h.

2.5 Preparation of the WPU/Cellulose Membranes

To obtain effective and flexible membranes, WPU was employed as modifier to mix with cellulose films. The WPU/cellulose membranes were prepared through soaking process according to the previous works [25,26]. Firstly, the prepared WPU film was dissolved in acetone to form diluted solution under stirring at room temperature. Secondly, the cellulose films were directly put into WPU solution, and then were taken out in 5 min. Colorless viscous membranes were obtained and then placed in an oven at 50°C, -0.01 kPa vacuum for slow evaporation of solvent for 3 h.

2.6 Characterization of the Prepared Celluloses and Their Composites

2.6.1 The Bulk Structure of the Prepared Samples

Fourier transform infrared (FTIR) spectroscopy measurement was used to identify the structure of WPU/CNC films. The infrared spectra of the WPU/CNC films were obtained with a Fourier Transform IR spectrophotometer (SHIMADZU FTIR-8400S [CE]) and recorded in the transmission mode at room temperature by averaging 40 scans at a resolution of 4.0 cm^{-1} . The spectra were analyzed in the frequency range of 4000–400 cm^{-1} . An X-ray diffraction instrument (XRD-7000, Shimadzu Limited, Japan) was used to analyze the crystallinity of the WUP/CNC films. A scanning of 2θ angle was in the range of 10 to 70° with the scan speed of 10.000 $\text{deg}\cdot\text{min}^{-1}$. X-ray Photoelectron Spectroscopy (XPS) was performed on an X-ray photoelectron spectrometer with a monochromatic focused Al $K\alpha$ X-ray source to determine C, N, O elements.

2.6.2 The Morphology of the Prepared Samples

The morphology of the prepared celluloses and their composites were investigated through scanning electron microscopy (SEM). SEM was performed using a SU-8010 microscope working at accelerating voltage of 1 kV. Before scanning, all the WPU/CNCs films were prepared with gold plating.

2.6.3 The Thermal and Mechanical Properties

Thermogravimetric analysis (TG) experiment was carried out under nitrogen atmosphere with NETZSCH TG209F3. WPU/CNCs film samples weighing from 4 to 10 mg were placed in an alumina ceramic crucible, and heated from 30 to 800°C under a heating rate of 10 °C/min. Differential scanning calorimetry (DSC) experiment was carried out in NETZSCH DSC200F3 equipment under nitrogen atmosphere with a temperature range from -80°C to 120°C, and two recycle was performed. The heating rate and cooling rate were 3 °C/min and the sample weight was 5–10 mg. The mechanical property and flexibility of the prepared membranes were investigated via a folding test on the instrument of controlling folding tester of Sichuan Changjiang Paper Instrument co., LTD. The folding speed is (175 ± 10) times/min, and the angle is $135^\circ \pm 2^\circ$. The detection was replicated for three times for each sample.

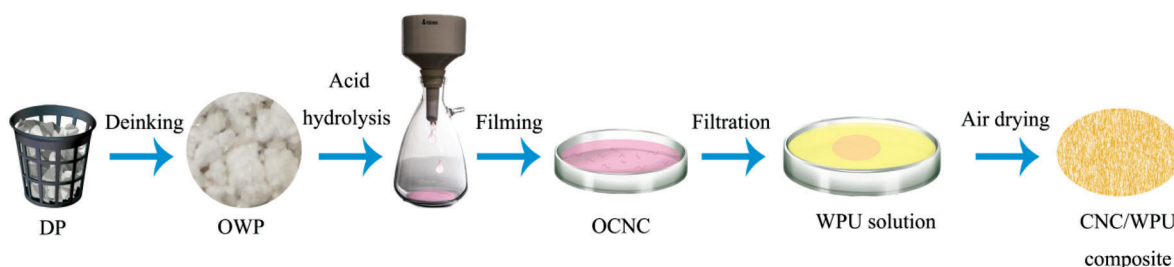
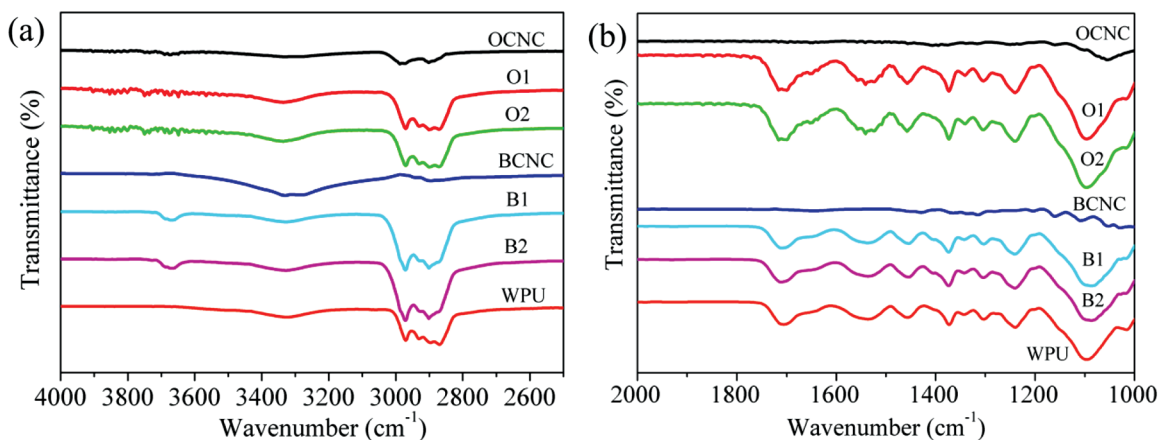
3 Results and Discussion

A series of celluloses and their composites with WPU were prepared via a facile process in this work. The samples information and abbreviations are listed in [Tab. 1](#). According to the previous works about the polyurethane and cellulose composites [24–26], the main weight and preparing parameters are also listed in [Tab. 1](#). The whole preparing process was illustrated in [Scheme 1](#).

FTIR was employed to identify the inner molecular structure and functional groups of the prepared CNC and the composites. As shown in [Fig. 1](#), the cellulose nanocrystals obtained from commercial cellulose (BCNC) and waste paper (OCNC) show the similar characteristic peaks at 3330 cm^{-1} , 2897 cm^{-1} , 1429 cm^{-1} and 1029 cm^{-1} , which can be attributed to the O–H, C–H, $-\text{CH}_2$ stretching vibration in polysaccharides and C–O–C pyranose ring stretching vibration, respectively. Notably, a band at 1645 cm^{-1} is obvious for OCNC, while the band disappear for BCNC. This may be the most important difference for the two kinds of CNC. The band may be attributed to the carbonyl (C=O) group, indicating that the

Table 1: Recipe, abbreviations and parameters for the preparation of celluloses and their composites

Composite	Fiber source	Weight of CNC/WPU (g)	Soaking time	Abbreviation
CNC	Commercial cellulose	1/0	None	BCNC
CNC + WPU	Commercial cellulose	1/2	20 s	B1
CNC + WPU	Commercial cellulose	1/2	5 min	B2
CNC	Office waste paper	1/0	None	OCNC
CNC + WPU	Office waste paper	1/2	20 s	O1
CNC + WPU	Office waste paper	1/2	5 min	O2

**Scheme 1:** The preparation process of the cellulose nanocrystals from waste paper and their combination with waterborne polyurethane**Figure 1:** FTIR spectra of the prepared CNC, WPU and their composites. (a) the main peaks in the range of 2600–4000 cm^{-1} ; (b) the main peaks in the range of 1000–1750 cm^{-1}

cellulose has been grafted with carboxyl group ($-\text{COOH}$) during the deinking and defibering of waste paper. This band appeared for the WPU/CNC composite, which arises from the $-\text{COO}^-$ in polyurethane [27,28]. This result suggests that the WPU has uniformly mixed with cellulose films. After the combination with the prepared WPU, the FTIR spectra of the composites are quite similar. For both the WPU and the composites, the main contribution in the range of 3000–3500 cm^{-1} can be ascribed to O-H stretching. The multiple peaks in the range of 1500–1750 cm^{-1} region are mainly attributed to the $-\text{NH}$ and $\text{C}=\text{O}$ from carbamate in WPU [29]. In addition, the main peaks located at 1500–1750 cm^{-1} and 3000–3700 cm^{-1} region for O1 and O2 samples are relatively broader than the other composites with BCNC, as well as the

WPU. Owing to the extra grafted carboxyl group for the OCNC, there may be much more hydrogen bond between OCNC and polyurethane than the WPU. Thus, we assume that the reason for the difference may be the high content of hydrogen bond. This interaction may cause wavenumbers to shift wider for the WPU/OCNC composites [26].

To further investigate the distribution and alignment of the polyurethane chains and CNC fibers, the X-ray diffraction (XRD) pattern of the CNC, WPU and their composites were detected. As shown in Fig. 2, WPU only had one broad peak at 19°, indicating that the prepared WPU was amorphous, corresponding to the previous work [30]. We found that the main diffraction peaks are almost the same to the CNC and WPU/CNC composites. The peaks of 2θ at 15° and 22° may be ascribed to the characteristics of the (110) and (002) lattice planes respectively for both the BCNC and OCNC. In addition, a weak and broad peak at about 34° can be observed on the curve of B1, which represented contribution of (040) plane attributed to typical cellulose nanocrystal structure. The appearance of these peaks suggests that WPU has been mixed with CNC significantly. Meanwhile, the main crystal structures of the prepared CNC did not change combining with WPU. To further analyze the difference of the crystal structures, the crystallinity index (CI) was calculated and used to compare the impact of the parameters and preparing process on the CNC and WPU/CNC composites. According to the previous report [31], the typical diffraction peak ca. $2\theta = 22^\circ$ can be used for the calculation of the CI by the following formula:

$$CI(\%) = \frac{I_{002} - I_{am}}{I_{002}} * 100 \quad (1)$$

where the I_{002} is the intensity of the (002) crystalline peak at around 22°, and I_{am} is the intensity for diffraction of non-crystalline material which is taken at 2θ of about 18° [18]. The values of CI for all the samples are shown in Tab. 2. It is clear that the BCNC and their composites possess higher CI comparing with that of OCNC and their composites. This may indicate that the processing of CNC from waste paper may destroy the crystal structure and decrease the crystallinity. This result corresponds to the FTIR analysis about the increase of the carboxyl group content in OCNC since the increase of the organic degree commonly accompanying with the decrease of the regularity [32]. When mixed with WPU, the CI decreases slightly (except for sample B2). It suggests that the chains in amorphous WPU may interact with the CNC in some extent, such as hydrogen bond. In this way, some nanocrystals may swell in the polyurethane dispersion in soaking process because the (002) plane consists of layered sheets of cellulose chains [26,33], corresponding to the previous work [34].

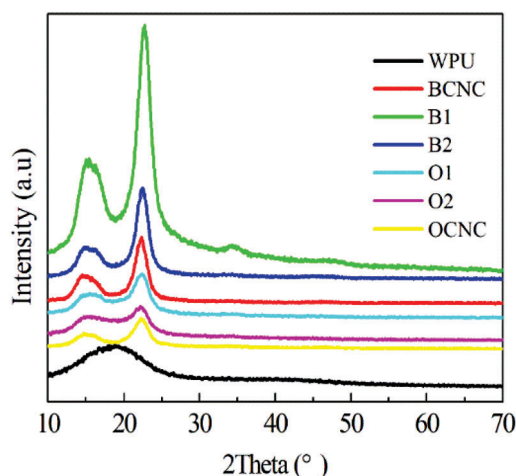


Figure 2: XRD spectra of the prepared CNC, WPU and their composites

Table 2: The values of CI for all the samples [35–37]

Samples	2 Θ (amorphous) ($^{\circ}$)	2 Θ (crystalline) ($^{\circ}$)	CI (%)
BCNC	14.6	22.3	56.14
B1	15.2	22.7	52.20
B2	15.1	22.5	62.53
OCNC	14.7	22.2	47.56
O1	15.0	22.4	41.34
O2	15.3	22.6	27.30

As depicted in Fig. 3, X-ray photoelectron spectra (XPS) were employed to detect the main elements and the carbon-based bonds of the CNC and WPU/CNC composites. The low-resolution spectra of both the BCNC and OCNC show the two main components including C and O elements in cellulose nanocrystals, and the three main elements of C, O and N in WPU. The all WPU/CNC composites (B1, B2, O1 and O2) present three main components, while the appearance of the nitrogen suggests the presence of polyurethane. The results indicate that the cellulose crystals have been mixed with polyurethane uniformly, corresponding to the results of FTIR and XRD.

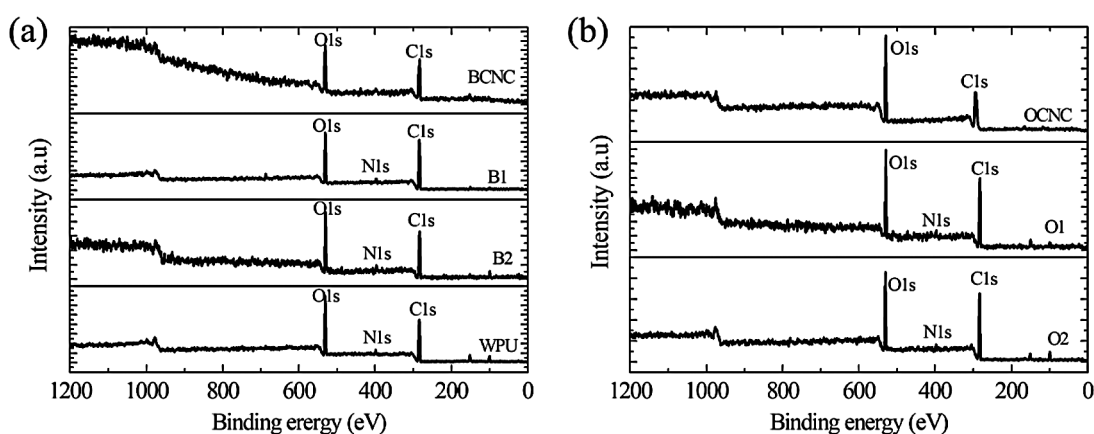


Figure 3: General XPS spectra for CNC, WPU and their composites (a) WPU, BCNC and their composites; (b) OCNC and their composites

The morphology details of the CNC and WPU/CNC composites were investigated by SEM, as shown in Fig. 4. It can be seen that both the BCNC and OCNC present a densely and evenly distributed of cellulose nanocrystals from the top surface view. It suggests that the cellulose nanocrystals have piled together to form dense membranes. Meanwhile, it seems that the piled cellulose crystals may form orientational structure as illustrated in the inset diagrams in Figs. 4a and 4d. On the basis of these dense films, we soaked them with polyurethane to form flexible membranes. It is clear that the cellulose nanocrystals have been uniformly coated with polyurethane and showed in Figs. 4b–4c and 4e–4f. Comparing with the polyurethane surface, the typical sea-island structure of polyurethane surface [27,28,38] can also be observed in the WPU/CNC composites, indicating that the cellulose nanocrystals have been shrouded by polyurethane chains. The inset high-resolution images also show that the cellulose nanocrystals have been covered completely. Notably, a distinct morphology of the B2 illustrates a corrugated and fiber-like surface. This unique surface is significantly similar with that of BCNC, while the B1, O1 and O2 only present the

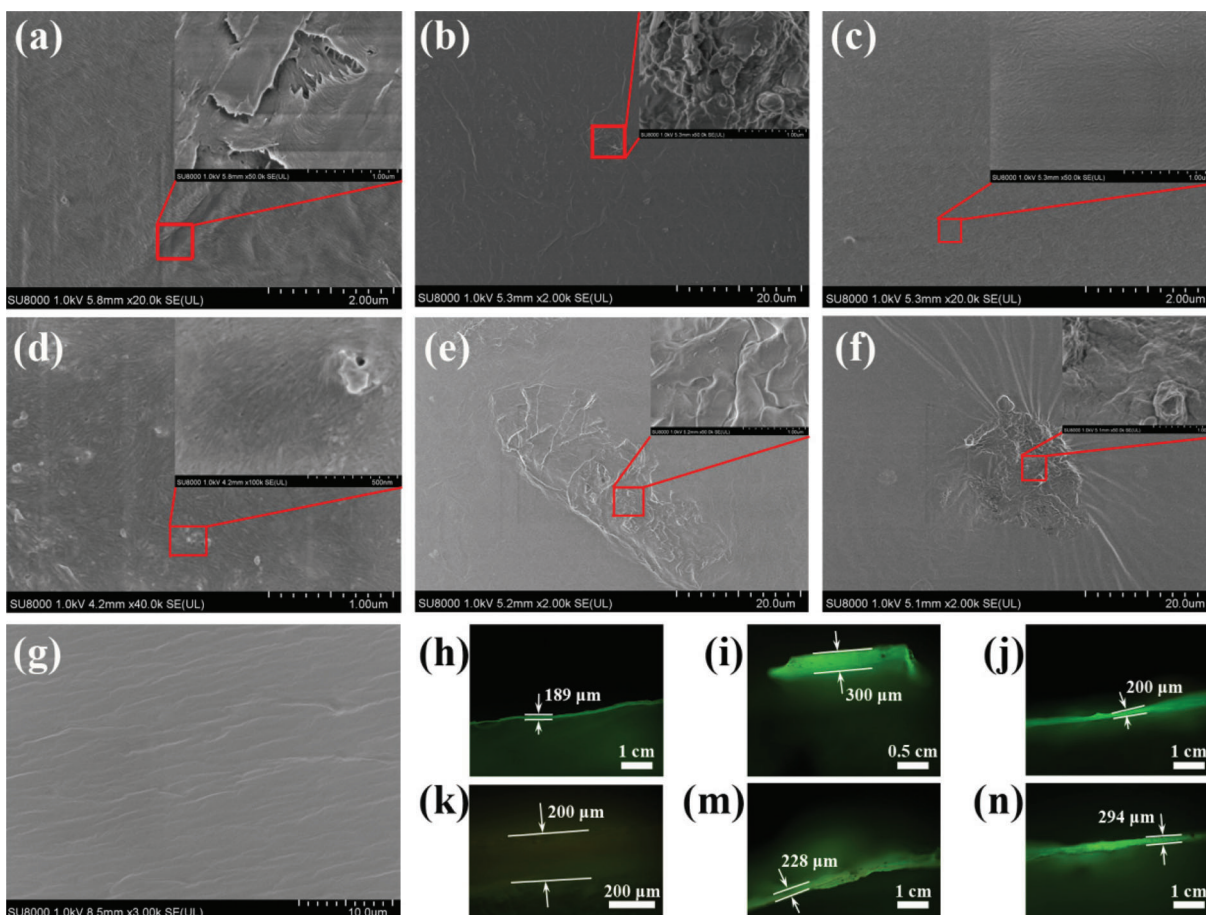


Figure 4: SEM images of CNC, WPU and their composites (a) BCNC, (b) B1, (c) B2, (d) OCNC, (e) O1, (f) O2 (the inset images in a–f are the high-resolution SEM morphologies of each sample), (g) WPU, (h–n) the microscopy images with the thickness of the prepared films

polyurethane surface. This difference may indicate that there is no correlation between the soaking time and absorbance of polyurethane on CNC films. In SEM images, it is vividly obvious that the dense CNC surface has been totally covered with polyurethane coatings in an irregular manner. The colorless and flexible membrane has been obtained by mixing with WPU, as shown in Fig. 4. It is obvious that the appearance of the membrane changes little after mixing with WPU. Meanwhile, the addition of WPU in CNC may increase the flexibility of the membrane. The cross-sectional surface was observed under a microscopy to compare the thickness of the prepared films, as shown in Fig. 4h–4n. The thickness of the BCNC and OCNC are about 189 μm and 200 μm , respectively, indicating that the prepared CNC from waste paper can form the similarly thin and dense film with commercial CNC. The thickness of the B1, B2, O1 and O2 are about 300 μm , 200 μm , 228 μm and 294 μm , respectively, as depicted in Fig. 4. It is obvious that the thickness of the composite films are improved, indicating further the absorbance of the polyurethane [39–41].

To further confirm the contribution of the WPU to the mechanical property of the CNC film. The folding test was performed, and the data was illustrated in Fig. 5. The folding endurance and flexibility of the WPU/CNC membranes have largely increased. In this study, the BCNC can only be folded once, while the OCNC can be folded ca. 20 times. The higher folding endurance of the OCNC may be due to the degradation of the waste paper. In preparing OCNC, the waste paper has been handled with various agents, especially acid and

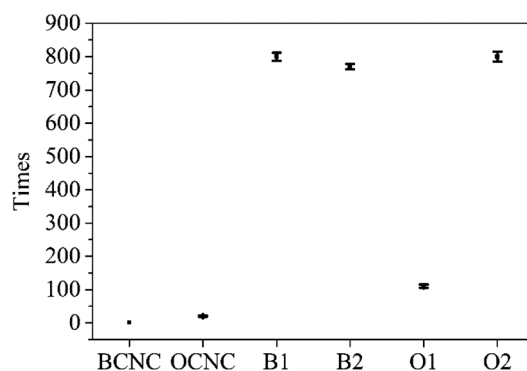


Figure 5: The folding test data of the CNC, WPU and their composites

alkaline. During the processes, the cellulose fibers may be damaged, as well as the cellulose nanocrystals. This has also been attested from the relative high carboxyl groups in OCNC by the FTIR analysis. Meanwhile, it is observed that the integrality of the nanocrystals in OCNC is not lower than that of BCNC, as shown in Figs. 4a and 4d. Therefore, the brittleness of the BCNC film may be higher than that of OCNC. When the WPU was mixed with CNC film, the B1, B2, O1 and O2 can be folded ca. 800, 770, 110 and 800 times respectively under a tension of 4.9 N. The results indicate that the BCNC may adsorb polyurethane in short time to form homogenous membrane with significant folding endurance, while the OCNC may adsorb polyurethane slowly and present a significant folding endurance until soaking enough time in polyurethane solution. This may also arise from the relative high content of carboxyl groups in OCNC and their composites [21]. Therefore, the mechanical properties of WPU/CNC composite membranes are significantly better than that of CNC based films, indicating great potential application as flexible materials [23].

After the folding test, the fractured surfaces of the composites were investigated by SEM detection, as shown in Fig. 6. Some fibers of the CNC can be observed in sample B1, O1 and O2, demonstrating the mixing of cellulose with WPU. Meanwhile, the fibers mainly aggregate together to present layer structure with the WPU film on the opposite sides, liking a sandwich structure. It suggests that WPU dispersions are mainly absorbed onto the surface of the CNC films. After the soaking in WPU dispersion, the CNC films keep a whole macrostructure and good appearance. As illustrated in Figs. 6a–6f, the CNC and composite films present significant transparency and extended appearance. In addition, the OCNC can also form an integrated film with scale and high transparency, as illustrated in Fig. 6b. After the absorbance of WPU, the film (sample B2) can even be folded in double back for several times manually, as depicted in Fig. 6g. As known, the pure CNC film is commonly brittle and hard to fold [42,43]. Thus, the addition of WPU may help to conquer the defects of the CNC film on mechanical property with little change of appearance and transparency [42].

Thermal properties of the CNC and WPU/CNC composites were evaluated by thermogravimetric analysis (TGA) in an inert N₂ atmosphere from 30 to 800°C. The thermal curves of the CNC film and their composites are depicted in Fig. 7, and the degradation information varying with temperature are listed in Tab. 3. It is clear that the WPU/CNC composites displayed higher thermal stability than CNC, indicating that polyurethane contributes to the thermal resistance for cellulose [44]. The specific decomposition peaks for all samples are illustrated in the derivative weight loss curve of DTG in Fig. 7b. According to our previous work about the WPU degradation in TGA analysis [27], the three stages can be ascribed to the residual water (mainly the hydration water), soft segment and hard segment of polyurethane, respectively, as shown in Tab. 3. It is obvious that there are also three major stages for BCNC and OCNC. The first temperature point is 141.6°C and 165.6°C respectively, which may be

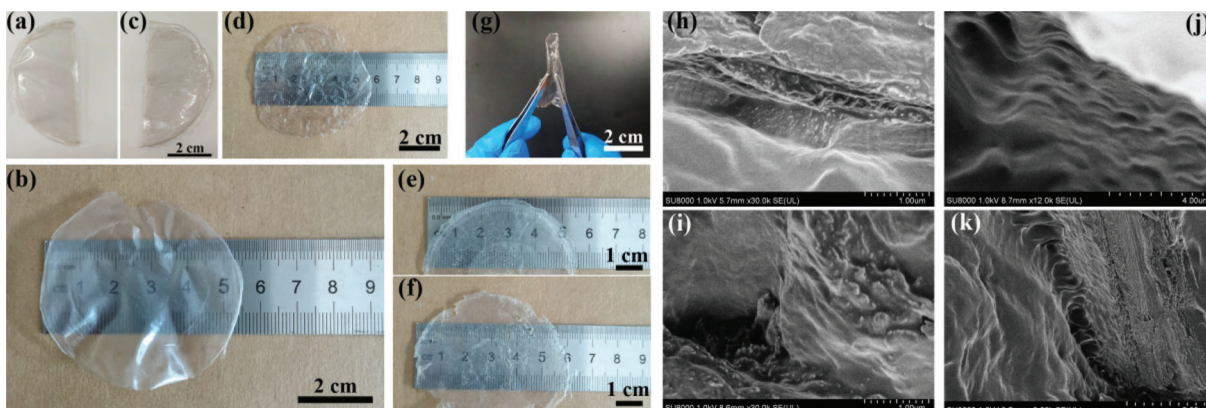


Figure 6: The digital and fractured surface images of the CNC/WPU composites (a–f) the digital photos of the BCNC, OCNC, B2, B1, O1 and O2; (g) manual folding test of sample B2; (h–k) the fractured surface morphology of the B1, O1, B2 and O2

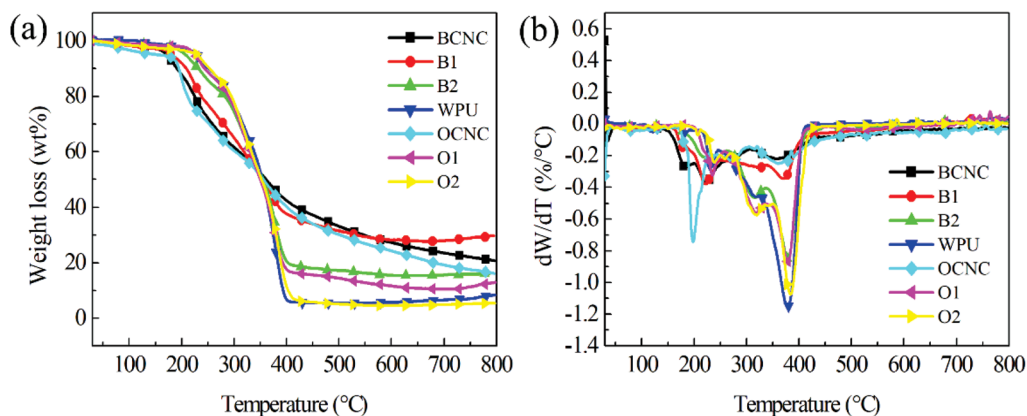


Figure 7: The TGA curves of the CNC, WPU and their composites (a) TG; (b) DTG

Table 3: The weight loss information varying with temperature

Sample	First decomposition		Second decomposition		Third decomposition	
	T1 (°C)	Weight loss (wt %)	T2 (°C)	Weight loss (wt %)	T3(°C)	Weight loss (wt %)
WPU	107.3	3.4	212.3	30.5	324.8	57.9
BCNC	141.6	12.2	199.3	27.4	307.9	39.6
OCNC	165.6	28.4	242.3	11.9	302.9	43.6
B1	152.5	21.1	246.2	24.3	338.8	24.9
B2	158.5	16.9	264.1	25.2	337.6	41.6
O1	189.5	12.8	258.1	31.1	336.7	43.3
O2	192.3	13.5	270.1	35.5	350.4	45.6

T1, T2 and T3 are the initial decomposition temperature

related to the loosely bound evaporation of water in combination with cellulose. The second degradation temperature is 199.3°C and 242.3°C respectively, which can be attributed to the degradation of CNC amorphous region. Notably, the second degradation temperature of the OCNC was high than that of BCNC, indicating that the thermal resistance of the amorphous region in cellulose nanocrystals from the waste paper is better than that of the commercial cellulose. This may also attest that the bulk structure of cellulose nanocrystals from waste paper was not so integrated comparing with that from commercial cellulose. It suggests that more amorphous structure may be generated because of the higher acid and other degradation agents. The third degradation stage is 307.9°C and 302.9°C, respectively, which may be connected with the breakdown of crystal interior. The decomposition temperature of BCNC is higher than that of OCNC, which indicates that the stability of commercial cellulose in this stage is better than that of prepared cellulose nanocrystals. When mixed with polyurethane, the thermal resistance of the WPU/CNC composites increased significantly. The initial degradation temperature of the first stage may be the most effective index to reflect the thermal resistance of the material. As listed in Tab. 3, the initial degradation temperatures of sample B1 and B2, O1 and O2 are higher than that of BCNC and OCNC, respectively. It implies that the addition of polyurethane benefits to the thermal resistance of the CNC film. This may be because urethane and urea of polyurethane can resist the damage of polymer chain, thus improving the thermal stability of CNC [45]. Additionally, the initial degradation temperature of the B2 (158.5°C) and O2 (192.3°C) are slightly higher than that of B1 (152.5°C) and O1 (189.5°C) respectively, indicating that the degradation temperature enhanced with the increase of the soaking time.

To further investigate the thermal behavior of the CNC and their composites, the DSC thermograms was performed. As shown in Fig. 8, it is obvious that a distinct endotherm peak attributing to an indication of the thermally decomposes of the crystalline packed cellulose for both BCNC and OCNC. As the temperature increases, the distinct endotherm peak which can be ascribed to the degradation of CNC can be observed at ca. 150°C, corresponding to the result in TGA analysis. A glass transition temperature belonging to soft segment in WPU can be seen in the range from -70°C to -40°C, and another endotherm peak at about 218°C may be ascribed to the decomposition point according to the TGA results [27]. It is obvious that the decomposed temperatures of celluloses (both BCNC and OCNC) are lower than WPU in DSC curves, and that of CNC/WPU composites are between CNC and WPU. This suggests that the addition of WPU may increase the thermal decomposed temperature, corresponding to the TGA results [46]. As a result, the mixing of WPU can effectively increase the thermal resistance of the CNC films, and cellulose crystals may interact moderately with polyurethane chains with little impact on the thermal behavior on the WPU/CNC composites.

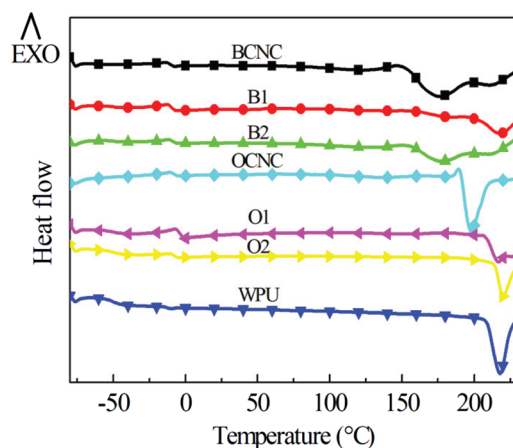


Figure 8: DSC diagrams of CNC, WPU and CNC/WPU films

4 Conclusion

Flexible polyurethane/cellulose nanocrystals composite membranes were prepared using the synthesized polyurethane and cellulose nanocrystals from waste paper through a facile process. It is found that the CNC obtained from waste paper may absorb polyurethane to form sandwich structure with significant appearance and transparency. We compared the obtained cellulose and CNC with the commercial cellulose with the origin film and their composite with polyurethane. It is found that the prepared cellulose nanocrystals from waste paper presents the similar quality to that from the commercial cellulose. The thermal resistance of the CNC from waste paper is higher than that from commercial cellulose of ca. 20°C. The cellulose nanocrystals from both the two resources can be mixed with polyurethane uniformly. The mixed membranes present a large increase in flexibility in folding test comparing with the CNC film, as well as the thermal resistance. The soaking time has little influence on the thermal resistance for both the BCNC and OCNC based composites. In addition, the composite from OCNC presents a better thermal resistance >30°C.

Funding Statement: The authors acknowledge the financial support provided by the National Natural Science Foundation of China [Grant No. 51802259], China Postdoctoral Science Foundation Funded Project [Grant No. 2019M663785], the Natural Science Foundation of Shaanxi [Grant No. 2019JQ-510], the Natural Science Basic Research Plan in Shaanxi Province of China [Grant No. 2018JM5053], Xi'an and Xi'an Beilin District Programs for Science and Technology Plan [Grant No. 201805037YD15CG21(18) and GX1913], the Promotion Program for Youth of Shaanxi University science and technology association [Grant No. 20190415], Fund of Key laboratory of Processing and Quality Evaluation Technology of Green Plastics of China National Light Industry council [Grant No. PQETGP2019003], the Ph.D. Start-up fund project [Grant No. 108-451118001] of Xi'an University of Technology.

Conflicts of Interest: The authors declare that they have no conflicts of interest to report regarding the present study.

References

1. Zhang, C., Garrison, T. F., Madbouly, S. A., Kessler, M. R. (2017). Recent advances in vegetable oil-based polymers and their composites. *Progress in Polymer Science*, 71, 91–143. DOI 10.1016/j.progpolymsci.2016.12.009.
2. Liang, H. Y., Liu, L. X., Lu, J. G., Chen, M. T., Zhang, C. Q. (2018). Castor oil-based cationic waterborne polyurethane dispersions: storage stability, thermo-physical properties and antibacterial properties. *Industrial Crops and Products*, 117, 169–178. DOI 10.1016/j.indcrop.2018.02.084.
3. Joshi, G., Naithani, S., Varshney, V. K., Bisht, S. S., Rana, V. (2017). Potential use of waste paper for the synthesis of cyanoethyl cellulose: a cleaner production approach towards sustainable environment management. *Journal of Cleaner Production*, 142, 3759–3768. DOI 10.1016/j.jclepro.2016.10.089.
4. Antoinette, C. O. (1997). Cellulose: the structure slowly unravels. *Cellulose*, 4(3), 173–207. DOI 10.1023/A:1018431705579.
5. Angkuratipakorn, T., Sriprai, A., Tantrawong, S., Chaiyasit, W., Singkhonrat, J. (2017). Fabrication and characterization of rice bran oil-in-water Pickering emulsion stabilized by cellulose nanocrystals. *Colloids and Surfaces A: Physicochemical and Engineering Aspects*, 522, 310–319. DOI 10.1016/j.colsurfa.2017.03.014.
6. Zhang, T. T., Cheng, Q. Y., Ye, D. D., Chang, C. Y. (2017). Tunicate cellulose nanocrystals reinforced nanocomposite hydrogels comprised by hybrid cross-linked networks. *Carbohydrate Polymers*, 169, 139–148. DOI 10.1016/j.carbpol.2017.04.007.
7. El, A. M., Kassab, Z., Aboukas, A., Gaillard, C., Barakat, A. (2018). Reuse of red algae waste for the production of cellulose nanocrystals and its application in polymer nanocomposites. *International Journal of Biological Macromolecules*, 106, 681–691. DOI 10.1016/j.ijbiomac.2017.08.067.
8. Gong, X. Y., Wang, Y. X., Chen, L. Y. (2017). Enhanced emulsifying properties of wood-based cellulose nanocrystals as pickering emulsion stabilizer. *Carbohydrate Polymers*, 169, 295–303. DOI 10.1016/j.carbpol.2017.04.024.

9. Wang, Q. Q., Zhao, X., Zhu, J. Y. (2014). Kinetics of strong acid hydrolysis of a bleached kraft pulp for producing cellulose nanocrystals (CNCs). *Industrial & Engineering Chemistry Research*, 53(27), 11007–11014. DOI 10.1021/ie501672m.
10. Lin, W., Chen, D., Yong, Q., Huang, C., Huang, S. (2019). Improving enzymatic hydrolysis of acid-pretreated bamboo residues using amphiphilic surfactant derived from dehydroabietic acid. *Bioresource Technology*, 293, 122055. DOI 10.1016/j.biortech.2019.122055.
11. Wang, W. H., Du, G. H., Li, C., Zhang, H. J., Long, Y. D. et al. (2016). Preparation of cellulose nanocrystals from asparagus (*Asparagus officinalis* L.) and their applications to palm oil/water Pickering emulsion. *Carbohydrate Polymers*, 151, 1–8. DOI 10.1016/j.carbpol.2016.05.052.
12. Klemm, D., Kramer, F., Moritz, S., Lindstrom, T., Ankerfors, M. et al. (2011). Nanocelluloses: a new family of nature-based materials. *Angewandte Chemie International Edition*, 50(24), 5438–5466. DOI 10.1002/anie.201001273.
13. Dipin, T., Jinitha, T. V., Purushothaman, E. (2019). Development of biocomposites of MCC extracted from non-wood sources. *Journal of Renewable Materials*, 7(11), 1109–1119. DOI 10.32604/jrm.2019.07636.
14. Gu, J., Pei, W., Tang, S., Yan, F., Peng, Z. et al. (2020). Procuring biologically active galactomannans from spent coffee ground (SCG) by autohydrolysis and enzymatic hydrolysis. *International Journal of Biological Macromolecules*, 149, 572–580. DOI 10.1016/j.ijbiomac.2020.01.281.
15. Chiromito, E. M. S., Trovatti, E., Carvalho, A. J. F. (2019). Water-based processing of fiberboard of acrylic resin composites reinforced with cellulose wood pulp and cellulose nanofibrils. *Journal of Renewable Materials*, 7(5), 403–412. DOI 10.32604/jrm.2019.01846.
16. Trache, D., Hussin, M. H., Haafizc, M. K. M., Thakur, V. K. (2017). Recent progress in cellulose nanocrystals: sources and production. *Nanoscale*, 9(5), 1763–1786. DOI 10.1039/C6NR09494E.
17. Kamel, S., Haroun, A. A., El, N. A. M., Diab, M. A. (2019). Electroconductive composites containing nanocellulose, nanopolypyrrole, and silver nanoparticles. *Journal of Renewable Materials*, 7(20), 193–203. DOI 10.32604/jrm.2019.00144.
18. Lei, W. Q., Fang, C. Q., Zhou, X., Yin, Q., Pan, S. F. et al. (2018). Cellulose nanocrystals obtained from office waste paper and their potential application in PET packing materials. *Carbohydrate Polymers*, 181, 376–385. DOI 10.1016/j.carbpol.2017.10.059.
19. Branciforti, M. C., Bellani, C. F., Morelli, C. L., Ferrand, A. F., Benkirane, J. N. et al. (2019). Poly (Butylene Adipate-Co-Terephthalate) and Poly (ϵ -Caprolactone) and their bionanocomposites with cellulose nanocrystals: thermo-mechanical properties and cell viability study. *Journal of Renewable Materials*, 7(3), 269–277. DOI 10.32604/jrm.2019.01833.
20. Chaabouni, O., Boufi, S. (2017). Cellulose nanofibrils/polyvinyl acetate nanocomposite adhesives with improved mechanical properties. *Carbohydrate Polymers*, 156, 64–70. DOI 10.1016/j.carbpol.2016.09.016.
21. Zhou, X., Su, J., Wang, C., Fang, C., He, X. et al. (2020). Design, preparation and measurement of protein/CNTs hybrids: a concise review. *Journal of Materials Science & Technology*, 46, 74–87. DOI 10.1016/j.jmst.2020.01.008.
22. Liang, H. Y., Wang, S. W., He, H., Wang, M. Q., Liu, L. X. et al. (2018). Aqueous anionic polyurethane dispersions from castor oil. *Industrial Crops and Products*, 122, 182–189. DOI 10.1016/j.indcrop.2018.05.079.
23. Zhou, X., Li, Y., Fang, C. Q., Li, S. J., Cheng, Y. L. et al. (2015). Recent advances in synthesis of waterborne polyurethane and their application in water-based Ink: a review. *Journal of Materials Science & Technology*, 31(7), 708–722. DOI 10.1016/j.jmst.2015.03.002.
24. Das, P., Malho, J. M., Rahimi, K., Schacher, F. H., Wang, B. et al. (2015). Nacre-mimetics with synthetic nanoclays up to ultrahigh aspect ratios. *Nature Communications*, 6(1), 5967. DOI 10.1038/ncomms6967.
25. Riaz, T., Ahmad, A., Saleemi, S., Adrees, M., Jamshed, F. et al. (2016). Synthesis and characterization of polyurethane-cellulose acetate blend membrane for chromium (VI) removal. *Carbohydrate Polymers*, 153, 582–591. DOI 10.1016/j.carbpol.2016.08.011.

26. Li, Y., Chen, H., Liu, D., Wang, W., Liu, Y. et al. (2015). pH-Responsive shape memory Poly (ethylene glycol)-Poly(ϵ -caprolactone)-based polyurethane/Cellulose nanocrystals nanocomposite. *ACS Applied Materials & Interfaces*, 7(23), 12988–12999. DOI 10.1021/acsami.5b02940.
27. Zhou, X., Fang, C. Q., Lei, WQ., Su, J., Li, L. et al. (2017). Thermal and crystalline properties of waterborne polyurethane by in situ water reaction process and the potential application as biomaterial. *Progress in Organic Coatings*, 104, 1–10. DOI 10.1016/j.porgcoat.2016.12.001.
28. Zhou, X., Fang, C. Q., Lei, W. Q., Du, J., Huang, T. et al. (2016). Various nanoparticle morphologies and surface properties of waterborne polyurethane controlled by water. *Scientific Reports*, 6(1), 34574. DOI 10.1038/srep34574.
29. Zhou, X., Fang, C. Q., He, X. Y., Wang, Y. Z., Yang, J. et al. (2017). The morphology and structure of natural clays from Yangtze River and their interactions with polyurethane elastomer. *Composites Part A: Applied Science and Manufacturing*, 96, 46–56. DOI 10.1016/j.compositesa.2017.02.009.
30. Zhou, X., Fang, C. Q., Yu, Q., Yang, R., Xie, L. et al. (2017). Synthesis and characterization of waterborne polyurethane dispersion from glycolized products of waste polyethylene terephthalate used as soft and hard segment. *International Journal of Adhesion and Adhesives*, 74, 49–56. DOI 10.1016/j.ijadhadh.2016.12.010.
31. Segal, L., Greely, J. J., Martin, A. E., Conrad, C. M. (1959). An empirical method for estimating the degree of crystallinity of native cellulose using the X-ray diffractometer. *Textile Research Journal*, 10(10), 786–794. DOI 10.1177/004051755902901003.
32. Tan, X. Y., Hamid, S. B. A., Lai, C. W. (2015). Preparation of high crystallinity cellulose nanocrystals (CNCs) by ionic liquid solvolysis. *Biomass and Bioenergy*, 81, 584–591. DOI 10.1016/j.biombioe.2015.08.016.
33. Hassana, M. L., Moorefieldb, C. M., Elbatal, H. S., Newkomeb, G. R., Modarellid, D. A. et al. (2012). Fluorescent cellulose nanocrystals via supramolecular assembly of terpyridine-modified cellulose nanocrystals and terpyridine-modified perylene. *Materials Science and Engineering: B*, 177(4), 350–358. DOI 10.1016/j.mseb.2011.12.043.
34. Ahvenainen, P., Kontro, I., Svedström, K. (2016). Comparison of sample crystallinity determination methods by X-ray diffraction for challenging cellulose I materials. *Cellulose*, 23(2), 1073–1086. DOI 10.1007/s10570-016-0881-6.
35. Park, N. M., Choi, S., Oh, E. J., Hwang, D. Y. (2019). Facile extraction of cellulose nanocrystals. *Carbohydrate Polymers*, 223, 115114. DOI 10.1016/j.carbpol.2019.115114.
36. Huang, C., Wang, X., Liang, C., Jiang, X., Yang, G. et al. (2019). A sustainable process for procuring biologically active fractions of high-purity xylooligosaccharides and water-soluble lignin from Moso bamboo prehydrolyzate. *Biotechnology for Biofuels*, 12(1), 189. DOI 10.1186/s13068-019-1527-3.
37. Dong, H., Zheng, L., Yu, P., Jiang, Q., Wu, Y. et al. (2020). Characterization and application of lignin-carbohydrate complexes from lignocellulosic materials as antioxidants for scavenging *in vitro* and *in vivo* reactive oxygen species. *ACS Sustainable Chemistry & Engineering*, 8(1), 256–266. DOI 10.1021/acssuschemeng.9b05290.
38. Zia, K. M., Anjum, S., Zuber, M., Mujahid, M., Jamil, T. (2014). Synthesis and molecular characterization of chitosan based polyurethane elastomers using aromatic diisocyanate. *International Journal of Biological Macromolecules*, 66, 26–32. DOI 10.1016/j.ijbiomac.2014.01.073.
39. Zhou, X., Deng, J., Fang, C., Yu, R., Lei, W. et al. (2020). Preparation and characterization of lysozyme@carbon nanotubes/waterborne polyurethane composite and the potential application in printing inks. *Progress in Organic Coatings*, 142, 105600. DOI 10.1016/j.porgcoat.2020.105600.
40. Liang, H., Li, Y., Huang, S., Huang, K., Zeng, X. et al. (2020). Tailoring the performance of vegetable oil-based waterborne polyurethanes through incorporation of rigid cyclic rings into soft polymer networks. *ACS Sustainable Chemistry & Engineering*, 8(2), 914–925. DOI 10.1021/acssuschemeng.9b05477.
41. Zhang, Y., Zhang, W., Wang, X., Dong, Q., Zeng, X. et al. (2020). Waterborne polyurethanes from castor oil-based polyols for next generation of environmentally-friendly hair-styling agents. *Progress in Organic Coatings*, 142, 105588. DOI 10.1016/j.porgcoat.2020.105588.
42. Zhou, X., Deng, J., Yang, R., Zhou, D., Fang, C. et al. (2020). Facile preparation and characterization of fibrous carbon nanomaterial from waste polyethylene terephthalate. *Waste Management*, 107, 172–181. DOI 10.1016/j.wasman.2020.03.041.

43. Lei, W. Q., Zhou, X., Fang, C. Q., Song, Y. H., Li, Y. G. (2019). Eco-friendly waterborne polyurethane reinforced with cellulose nanocrystal from office waste paper by two different methods. *Carbohydrate Polymers*, 209, 299–309. DOI 10.1016/j.carbpol.2019.01.013.
44. Lei, W. Q., Fang, C. Q., Zhou, X., Li, Y., Pu, M. Y. (2018). Polyurethane elastomer composites reinforced with waste natural cellulosic fibers from office paper in thermal properties. *Carbohydrate Polymers*, 197, 385–394. DOI 10.1016/j.carbpol.2018.06.036.
45. Sehaqui, H., Kulasinski, K., Pfenninger, N., Zimmermann, T., Tingaut, P. (2017). Highly carboxylated cellulose nanofibers via succinic anhydride esterification of wheat fibers and facile mechanical disintegration. *Biomacromolecules*, 18(1), 242–248. DOI 10.1021/acs.biomac.6b01548.
46. Santamaria, E. A., Fernandes, I., Ugarte, L., Barreiro, F., Arbelaiz, A. et al. (2018). Waterborne polyurethane-urea dispersion with chain extension step in homogeneous medium reinforced with cellulose nanocrystal. *Composites Part B: Engineering*, 137, 31–38. DOI 10.1016/j.compositesb.2017.11.004.